

# Simulation Studies of Detrapping of Ultrarelativistic Electrons from an Oblique Shock Wave due to Multidimensional Fluctuations<sup>\*)</sup>

Mieko TOIDA and Junya JOHO

*Department of Physics, Nagoya University, Nagoya 464-8602, Japan*

(Received 16 November 2012 / Accepted 14 March 2013)

A magnetosonic shock wave propagating obliquely to an external magnetic field can trap and accelerate electrons to ultrarelativistic energies. These electrons can excite electromagnetic fluctuations along the shock front. The effects of the electromagnetic fluctuations on electron motion are investigated by two-dimensional electromagnetic particle simulations and test particle calculations in which equation of motion of electrons in the electromagnetic fields averaged along the shock front is computed. Comparisons of the two results verify that the electromagnetic fluctuations along the shock front can cause detrapping of energetic electrons from the main pulse and their subsequent acceleration to higher energies. It is also demonstrated that as the external magnetic field strengthens, the electromagnetic fluctuations along the shock front grow to larger amplitudes, and the detrapping and subsequent acceleration of electrons enhance.

© 2013 The Japan Society of Plasma Science and Nuclear Fusion Research

Keywords: particle acceleration, collisionless shock, trapping, detrapping, particle simulation

DOI: 10.1585/pfr.8.2401031

## 1. Introduction

High-energy electrons are often produced in astrophysical plasmas. For instance, in solar flares, electrons are accelerated to several tens of megaelectronvolts within a few seconds. It has been believed that the electrons are accelerated by shock waves.

Theory and one-dimensional (1D) electromagnetic particle simulations [1] showed that a magnetosonic shock wave propagating obliquely to an external magnetic field with a propagation speed  $v_{sh}$  close to  $c \cos \theta$ , where  $c$  is the speed of light and  $\theta$  is the propagation angle of the shock wave, can rapidly accelerate electrons to ultrarelativistic energies. According to the theory [2], the maximum Lorentz factor of the accelerated electrons can be estimated as

$$\gamma_m \sim \frac{|\Omega_e|^2}{\omega_{pe}^2} \frac{v_{sh} c \cos \theta}{v_A (c \cos \theta - v_{sh})}, \quad (1)$$

where  $\Omega_e (< 0)$  and  $\omega_{pe}$  are the electron gyro frequency and plasma frequency, respectively. As predicted by Eq. (1), the acceleration is enhanced in a strong magnetic field, and high-energy electrons with  $\gamma > 100$  have been observed in simulations with  $|\Omega_e|/\omega_{pe} > 1$ . This mechanism will thus be important in the generation of high-energy electrons in plasmas with strong magnetic fields such as solar magnetic tubes and pulsars.

author's e-mail: toida@cc.nagoya-u.ac.jp

<sup>\*)</sup> This article is based on the presentation at the 22nd International Toki Conference (ITC22).

In this mechanism, electrons are trapped and energized in the main pulse region of the shock wave. In the 1D simulations, once electrons are trapped, they cannot readily escape from the wave and are trapped deep in its main pulse region [3]. Recently, two-dimensional (2D), fully kinetic, relativistic, electromagnetic particle simulations have shown [4] that after trapping and energization in the main pulse, electrons can be detrapped from the main pulse, unlike in the 1D case. Some of the detrapped electrons have been observed to be accelerated to much higher energies by the mechanism reported in Ref. [5] for accelerating relativistic ions. This detrapping has been attributed to 2D electromagnetic fluctuations along the shock front, which are due to oblique whistler waves excited by relative motion between trapped and passing electrons.

In this paper, we study the effects of the 2D electromagnetic fluctuations on electron motion with 2D electromagnetic particle simulations and test particle calculations. First, we follow the orbits of a large number of electrons in a 2D electromagnetic particle simulation in which a shock wave is assumed to propagate in the  $x$  direction. Next, we calculate the motions of the same number of test electrons in the electromagnetic fields averaged along the  $y$  direction (1D fields), which are obtained from the 2D electromagnetic simulations. Comparisons of the two results confirm that the 2D electromagnetic fluctuations along the shock front can cause the detrapping of electrons from the main pulse region. We also study the dependence of electron detrapping on the strength of the external magnetic field

when the nonstationarity of the 1D fields remains small. We show that as  $|\Omega_e|/\omega_{pe}$  increases, the amplitude of the 2D electromagnetic fluctuations increases, and the detrapping and subsequent acceleration of electrons enhance.

## 2. Detrapping due to Electromagnetic Fluctuations

In this section, we briefly describe a physical picture for electron detrapping from an oblique shock wave [6]. Assuming that a shock wave propagates in the  $x$ -direction with a constant speed  $v_{sh}$  in an external magnetic field in the  $(x, z)$  plane,  $\mathbf{B}_0 = B_0(\cos\theta, 0, \sin\theta)$ , we write the electric and magnetic fields in a frame moving with the shock wave as

$$\mathbf{E}(x, y, z, t) = \bar{\mathbf{E}}(x, t) + \delta\mathbf{E}_2(x, y, z, t), \quad (2)$$

$$\mathbf{B}(x, y, z, t) = \bar{\mathbf{B}}(x, t) + \delta\mathbf{B}_2(x, y, z, t), \quad (3)$$

where  $\bar{\mathbf{E}}$  and  $\bar{\mathbf{B}}$  are  $\mathbf{E}$  and  $\mathbf{B}$  averaged along the shock front (that is, averaged over the  $y$ - and  $z$ -directions), respectively. We call  $\bar{\mathbf{E}}$  and  $\bar{\mathbf{B}}$  the 1D fields, and  $\delta\mathbf{E}_2$  and  $\delta\mathbf{B}_2$  the multi-dimensional fluctuations.

We also consider the nonstationarity of the 1D fields and express  $\bar{\mathbf{E}}$  and  $\bar{\mathbf{B}}$  as

$$\bar{\mathbf{E}}(x, t) = \mathbf{E}_{sh}(x) + \delta\mathbf{E}_1(x, t), \quad (4)$$

$$\bar{\mathbf{B}}(x, t) = \mathbf{B}_{sh}(x) + \delta\mathbf{B}_1(x, t), \quad (5)$$

where  $\mathbf{E}_{sh}$  and  $\mathbf{B}_{sh}$  are the time-averaged  $\bar{\mathbf{E}}$  and  $\bar{\mathbf{B}}$ , respectively, and  $\delta\mathbf{E}_1$  and  $\delta\mathbf{B}_1$  represent the nonstationarity of  $\bar{\mathbf{E}}$  and  $\bar{\mathbf{B}}$ . Substituting Eqs. (2)-(5) in the Maxwell equations, we find that  $\bar{B}_x$ ,  $E_{ysh}$ , and  $E_{zsh}$  are constants. Assuming that  $E_{ysh}$  and  $E_{zsh}$  are equal to  $E_y$  and  $E_z$ , respectively, for a 1D ( $\partial/\partial y = \partial/\partial z = 0$ ) stationary ( $\partial/\partial t = 0$ ) shock wave, we have  $E_{ysh} = E_{y0} = -v_{sh}B_{zsh0}/c$  and  $E_{zsh} = 0$ , where  $B_{zsh0}$  is  $B_{zsh}$  in the upstream region given by  $B_{zsh0} = B_0 \sin\theta/(1 - v_{sh}^2/c^2)^{1/2}$ .

According to the simulation results, the characteristic length and time of the variations in  $\delta\mathbf{E}_j$  and  $\delta\mathbf{B}_j$  ( $j = 1$  or  $2$ ) are much longer than the electron gyroradius and gyroperiod, respectively. Then, using drift approximation, we write the velocity of an electron trapped in the main pulse region as

$$\mathbf{v} = v_{\parallel}\mathbf{B}/B + c\mathbf{E} \times \mathbf{B}/B^2. \quad (6)$$

Here the  $\nabla B$ -drift (and other insignificant drift) and gyration velocity have been neglected, because the gyration velocity is not essential in this trapping and acceleration mechanism [2]. Substituting the values of  $\mathbf{E}_{sh}$  and  $\mathbf{B}_{sh}$  in Eq. (6) and using  $v_{sh} \approx c \cos\theta$ , we obtain  $v_x$  as

$$v_x \approx c(\delta f_{11} + \delta f_{12})B_0/B_{zsh}, \quad (7)$$

with

$$\delta f_{11} \approx \delta E_{y1}/B_0, \quad \delta f_{12} \approx (\delta B_{x2} + \delta E_{y2})/B_0, \quad (8)$$

where we have neglected the second-order terms of  $\delta\mathbf{E}_j$  and  $\delta\mathbf{B}_j$ . Equation (7) indicates that when the shock wave is 1D and stationary ( $\delta f_{11} = \delta f_{12} = 0$ ), the trapped electrons cannot readily escape from the main pulse because  $v_x \approx 0$ . However, if the magnitudes of  $\delta f_{11}$  and  $\delta f_{12}$  are not small,  $v_x \approx 0$  can break down. We can therefore expect that some electrons may be detrapped from the main pulse under the influence of the fluctuations  $\delta f_{11}$  and  $\delta f_{12}$ .

Previous 1D electromagnetic particle simulations [2, 3] investigated electron motions in oblique shock waves with the Alfvén Mach number  $M_A \sim 2$ . In this study, using a 2D electromagnetic particle code, we simulate shock waves with  $M_A \approx 2.3$ , for which the nonstationarity in the 1D fields is small. As described in Ref. [4], the multi-dimensional fluctuations  $\delta f_{12}$  can grow to large amplitudes because of oblique whistler-wave instabilities excited by relative motion between trapped and passing electrons. The instabilities also cause current filamentation, and nonlinear interaction of the current filaments enhances the growth of  $\delta f_{12}$ .

## 3. Particle Simulations and Test Particle Calculations

### 3.1 Method and parameters

We investigate electron motion in an oblique shock wave with two methods. One is a 2D (two spatial coordinates and three velocity components) relativistic electromagnetic particle code with full ion and electron dynamics. The other is a test particle calculation in which we compute the motions of test electrons in 1D fields  $\bar{\mathbf{E}}(x, t)$  and  $\bar{\mathbf{B}}(x, t)$  by integrating the relativistic equation of motion,

$$\frac{d\mathbf{P}}{dt} = -e\bar{\mathbf{E}}(x, t) - \frac{e}{c}\mathbf{v} \times \bar{\mathbf{B}}(x, t). \quad (9)$$

Here,  $\bar{\mathbf{E}}(x, t)$  and  $\bar{\mathbf{B}}(x, t)$  are the  $y$ -averaged fields of  $\mathbf{E}(x, y, t)$  and  $\mathbf{B}(x, y, t)$ , respectively, obtained in the 2D electromagnetic particle simulation where the simulation plane is  $(x, y)$  and the shock wave propagates in the  $x$  direction. Comparison of the two results clarifies the effects of the 2D fluctuations  $\delta\mathbf{E}_2$  and  $\delta\mathbf{B}_2$  on electrons, which are included in the 2D electromagnetic particle simulation and excluded in the test particle calculation.

For the 2D electromagnetic particle simulation, the system size is  $L_x \times L_y = 16384\Delta_g \times 256\Delta_g$ , where  $\Delta_g$  is the grid spacing. The total number of simulation particles is  $N \approx 1.1 \times 10^9$ . We follow the orbits of  $2.1 \times 10^6$  electrons, which we call 2Ds electrons. We also compute the orbits of the same number of test electrons following Eq. (9). We denote these test electrons as 1Dt electrons. The initial positions and velocities of the 1Dt electrons are exactly the same as those of the 2Ds electrons.

The other simulation parameters are as follows. The ion-to-electron mass ratio is  $m_i/m_e = 400$ . Light speed is  $c/(\omega_{pe}\Delta_g) = 4.0$ , and the electron and ion thermal velocities in the upstream region are  $v_{Te}/(\omega_{pe}\Delta_g) = 0.5$  and

$v_{Ti}/(\omega_{pe}\Delta_g) = 0.025$ , respectively. The external magnetic field in the  $(x, z)$  plane is  $\mathbf{B}_0 = B_0(\cos\theta, 0, \sin\theta)$ . Shock waves are excited as described in Ref. [4].

In Ref. 6, we have presented the results for the case of the external magnetic field strength  $|\Omega_e|/\omega_{pe} = 5$ , the propagation speed of the shock wave  $v_{sh} = 0.95c \cos\theta$ , and the Alfvén Mach number  $M_A = 2.3$ . These values of  $v_{sh}$  and  $M_A$  are close to those in previous 1D particle simulations, where electron deep trapping in an oblique shock wave was observed [2, 3]. As shown by Eq. (1),  $|\Omega_e|/\omega_{pe}$  is a key parameter for the electron trapping, and the maximum energy of trapped electrons increases with  $|\Omega_e|/\omega_{pe}$ . In this paper, we study the dependence of electron detrapping due to 2D fluctuations on the parameter  $|\Omega_e|/\omega_{pe}$ . We perform simulations for  $|\Omega_e|/\omega_{pe} = 3, 4, 5$ , and 6, fitting  $v_{sh} = 0.95c \cos\theta$  and  $M_A = 2.3$ . This enables us to observe electron motion in an oblique shock wave under the condition that the amplitudes of 1D fluctuations for the four cases are almost the same level.

### 3.2 Differences between 1Dt and 2Ds electrons

Before discussing the dependence of electron motion on  $|\Omega_e|/\omega_{pe}$ , we describe the differences between 1Dt and 2Ds electrons using the data for  $|\Omega_e|/\omega_{pe} = 5$ , for which we have set  $\theta = 54^\circ$  [6]. Figure 1 shows the electron phase space plots  $(x, \gamma)$  (where  $\gamma$  is the Lorentz factor), the profile of  $\bar{B}_z(x)$ , and the contour map of  $B_x$  in the  $(x, y)$  plane at  $\omega_{pe}t = 3360$ . A comparison of the top and middle panels clearly shows that the distribution of high-energy 2Ds electrons is different from that of 1Dt electrons. Some 1Dt electrons are trapped and energized in the main pulse region, and there are no energetic electrons outside the region. However, energetic 2Ds electrons exist in a wider region from the upstream region to the downstream region. The maximum  $\gamma$  of 2Ds electrons is  $\gamma \sim 800$ , which is higher than that of 1Dt electrons,  $\gamma \sim 400$ . This difference is caused by 2D fluctuations in the electromagnetic fields along the shock front. The bottom panel shows that the fluctuations in  $B_x$  have large amplitudes in the main pulse region. As described in Ref. [4], the 2D fluctuations are due to whistler wave instabilities excited by the trapped electrons and have grown to large amplitudes as a result of nonlinear interaction of current filaments. The 2D fluctuations can cause detrapping of 2Ds electrons from the main pulse region and subsequent acceleration by the shock wave.

Figure 2 shows the time variations in  $\gamma$  and the positions  $x - x_m$  of a 2Ds electron (black solid line) and a 1Dt electron (gray dashed line), where  $x_m$  is the position at which  $\bar{B}_z$  has its peak. Although the initial velocities and positions of 2Ds and 1Dt electrons are exactly the same, their orbits are completely different after they are trapped in the main pulse region at  $\omega_{pe}t \approx 250$ . The 1Dt electron continues to be trapped in the main pulse until the end of the simulation, whereas the 2Ds electron is detrapped from

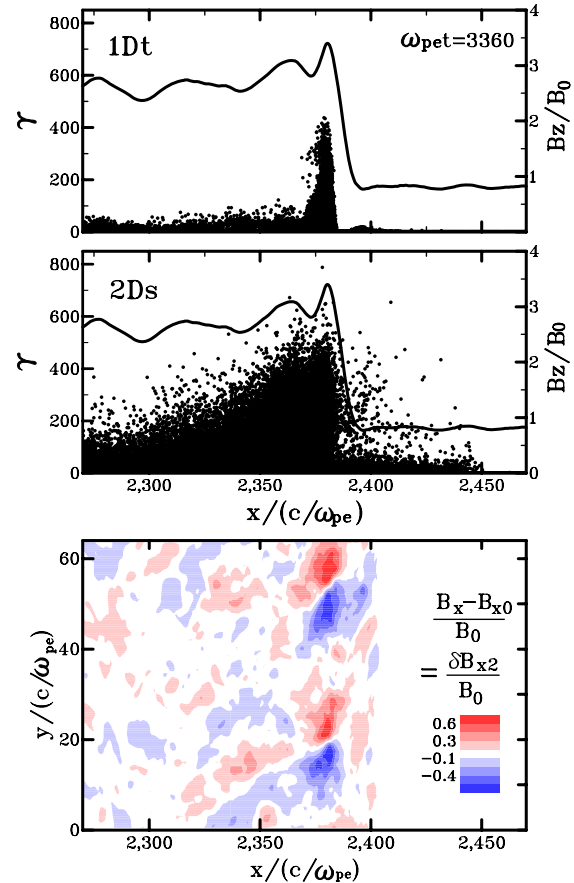


Fig. 1 Phase space plots  $(x, \gamma)$  of 1Dt and 2Ds electrons, profile of 1D magnetic field  $\bar{B}_z(x)$ , and contour map of  $B_x$  in the  $(x, y)$  plane at  $\omega_{pe}t = 3360$ .

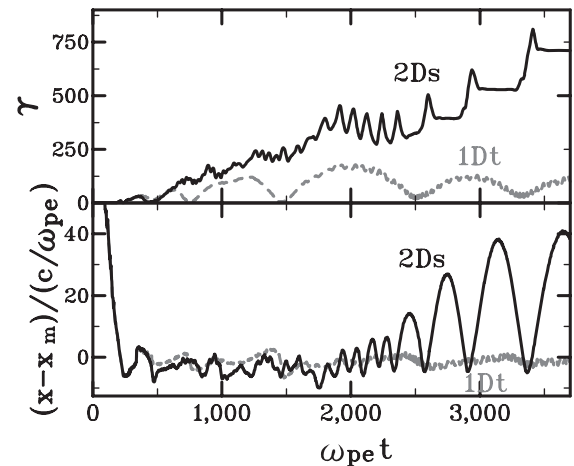


Fig. 2 Time variations in  $\gamma$  and the positions  $x - x_m$  of a 1Dt electron and a 2Ds electron with the same initial conditions.

it to the upstream region. The  $\gamma$  value of the 1Dt electron oscillates with a time period  $\omega_{pe}t \sim 1000$ , whereas the  $\gamma$  value of the 2Ds electron increases continuously on average. The 2Ds electron is energized to  $\gamma \sim 300$  in the main pulse region and departs with the high energy at

$\omega_{pe}t \approx 2500$ . Even after this, the 2Ds electron stays near the shock front. It then reenters the shock wave because of its gyromotion and is accelerated to a higher energy by the mechanism discussed in Ref. [5]. That is, it is accelerated by the transverse electric field  $E_y$  in the shock wave because the gyromotion is antiparallel to  $E_y$ . The energy increases once in the gyroperiod; the increment of  $\gamma$  is theoretically given by [5]

$$\delta\gamma \sim \alpha v_{\perp} \gamma, \quad (10)$$

where  $\alpha$  is a constant. This process repeats three times after  $\omega_{pe}t \approx 2500$ . The increment of  $\gamma$  at the third time ( $\omega_{pe}t \approx 3300$ ) is greater than that at earlier times (at  $\omega_{pe}t = 2500$  and  $2800$ ), which is consistent with Eq. (10).

We now show the relationship between the electromagnetic fluctuations and electron detrapping from the main pulse region. The upper panel in Fig. 3 displays the time variations in the numbers of 1Dt (gray dashed line) and 2Ds (black solid line) electrons that have been detrapped from the main pulse region. The lower panel shows the magnitudes of 1D (gray dashed line) and 2D (black solid line) fluctuations,  $\delta f_{11}$  and  $\delta f_{12}$ , defined by eq. (8), near the center of the main pulse, where  $|\delta f_{12}|$  is averaged along the  $y$  direction. A comparison of the upper and lower panels clearly shows that the detrapping of 2Ds electrons starts after the increase in  $|\delta f_{12}|$  (at  $\omega_{pe}t \sim 1000$ ). This indicates that the detrapping is caused by the 2D fluctuation. The amplitude of the 1D fluctuation  $\delta f_{11}$  remains small until the end of the simulation. Consequently, the number of detrapped 1Dt electrons is negligibly small.

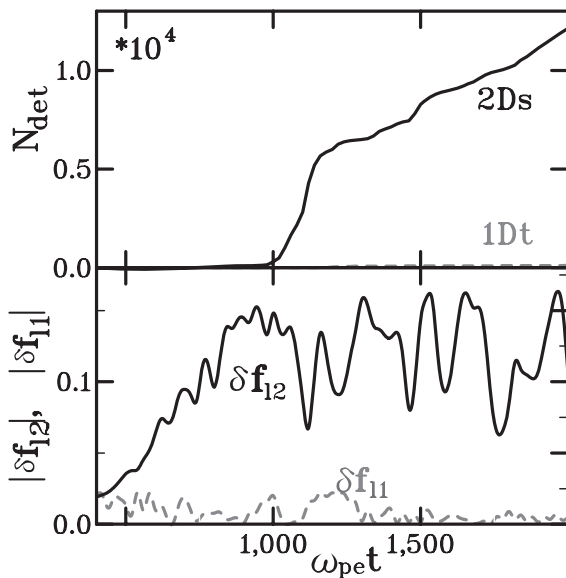


Fig. 3 Time variations in the numbers of 2Ds and 1Dt electrons that have been detrapped from the main pulse,  $N_{\text{det}}$ , and in the magnitudes of 2D fluctuation  $\delta f_{12}$  and 1D fluctuation  $\delta f_{11}$  in the main pulse region.

### 3.3 Dependence on external magnetic-field strength

We consider the dependence of the electron detrapping on the external magnetic-field strength if the 1D fluctuations are small. We perform simulations where  $|\Omega_e|/\omega_{pe}$  in the upstream region is 3, 4, 5, and 6, for which we have set  $\theta = 69^\circ, 61^\circ, 54^\circ$ , and  $45^\circ$ , respectively, to satisfy the relation  $v_{\text{sh}} \approx 0.95c \cos \theta$  and  $M_A = 2.3$  for all four cases. Figure 4 shows the time variations of the maximum Lorentz factor  $\gamma_{\text{max}}$  of the 1Dt electrons and the magnitudes of 2D fluctuations in the main pulse region for the cases of  $|\Omega_e|/\omega_{pe} = 3, 4, 5$ , and 6. The values are averaged over the period  $\omega_{pe}t = 250$ . Although  $v_{\text{sh}}$  increases with  $|\Omega_e|/\omega_{pe}$ , the electron trapping starts at  $\omega_{pe}t \approx 300$  and  $\gamma_{\text{max}}$  of the 1Dt electrons is saturated by  $\omega_{pe}t = 2000$  for all the four cases. The 2D fluctuations for the four  $|\Omega_e|/\omega_{pe}$ 's begin to grow at  $\omega_{pe}t \approx 300$  and are saturated by  $\omega_{pe}t = 2000$ .

We plot in Fig. 5 the energy distribution of 2Ds (black solid lines) and 1Dt (gray dashed lines) electrons at  $\omega_{pe}t = 3600$  for  $|\Omega_e|/\omega_{pe} = 3, 4, 5$ , and 6. Figure 5 and the upper panel in Fig. 4 show that as  $|\Omega_e|/\omega_{pe}$  increases, the maximum energy of the 1Dt electrons increases, which is consistent with the theory (Eq. (1)) for the electron acceleration in a 1D stationary shock wave. This indicates that as  $|\Omega_e|/\omega_{pe}$  increases, 2Ds electrons can be accelerated to higher energies in the main pulse and may retain their energies when they are detrapped from it. Then, the subsequent acceleration would produce a greater increment in  $\gamma$ , as predicted by Eq. (10). The difference between the maximum energies of the 2Ds and 1Dt electrons, which

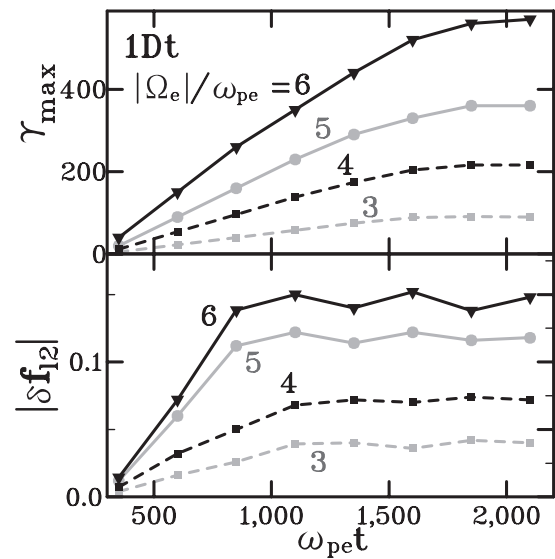


Fig. 4 Time variations of the maximum Lorentz factor  $\gamma_{\text{max}}$  of 1Dt electrons and the magnitudes of 2D fluctuations in the main pulse region for the cases of  $|\Omega_e|/\omega_{pe} = 3, 4, 5$  and 6. The values are averaged over the period  $\omega_{pe}t = 250$ .

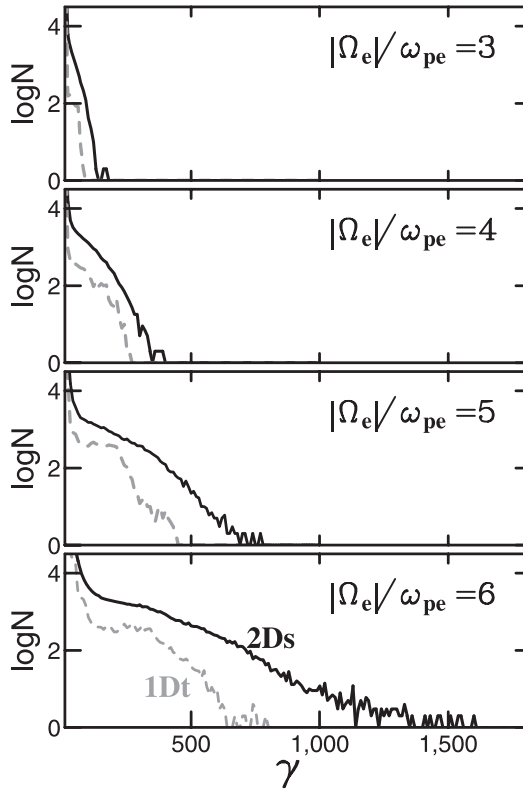


Fig. 5 Energy distribution of 1Dt and 2Ds electrons at  $\omega_{pe}t = 3600$  for  $|\Omega_e|/\omega_{pe} = 3, 4, 5,$  and  $6$ . The relations  $v_{sh} \approx 0.95c \cos \theta$  and  $M_A = 2.3$  are satisfied for all the cases.

is caused by the subsequent acceleration, would therefore increase as  $|\Omega_e|/\omega_{pe}$  increases. This is clearly shown in Fig. 5. We also note that the number of 2Ds electrons with energies higher than the maximum energy of the 1Dt electrons also increases with  $|\Omega_e|/\omega_{pe}$ . This indicates that electron detrapping is enhanced in a strong magnetic field.

Indeed, the number of detrapped 2Ds electrons increases with  $|\Omega_e|/\omega_{pe}$ , as shown in the middle panel of Fig. 6, where the numbers of 2Ds electrons that escaped from the main pulse by  $\omega_{pe}t = 3600$  are plotted. The values of  $N_{det}$  are normalized to the number of 2Ds electrons that encountered the shock wave by that time,  $N_{enc}$ . The numbers of detrapped 1Dt electrons are negligible. The upper panel in Fig. 6 shows the magnitudes of the 1D (gray triangles) and 2D (black circles) electromagnetic fluctuations,  $|\delta f_{i1}|$  and  $|\delta f_{i2}|$ , in the main pulse region averaged over the period from  $\omega_{pe}t = 500$  to  $3600$ . In all four cases, the 1D fluctuations remain small until the end of the simulation, whereas the 2D fluctuations grow to large amplitudes. As  $|\Omega_e|/\omega_{pe}$  increases, the magnitude of  $\delta f_{i2}$  increases, which enhances the electron detrapping. The bottom panel in Fig. 6 shows the numbers of 2Ds and 1Dt electrons that got trapped in the main pulse by  $\omega_{pe}t = 3600$ , normalized to  $N_{enc}$ . As  $|\Omega_e|/\omega_{pe}$  increases,  $v_{sh}$  and  $N_{enc}$  increases. However, the ratio  $N_{trap}/N_{enc}$  of the 1Dt electrons is almost independent of  $|\Omega_e|/\omega_{pe}$ . This is because the magnitudes of the 1D fluctuations for the four  $|\Omega_e|/\omega_{pe}$ 's are

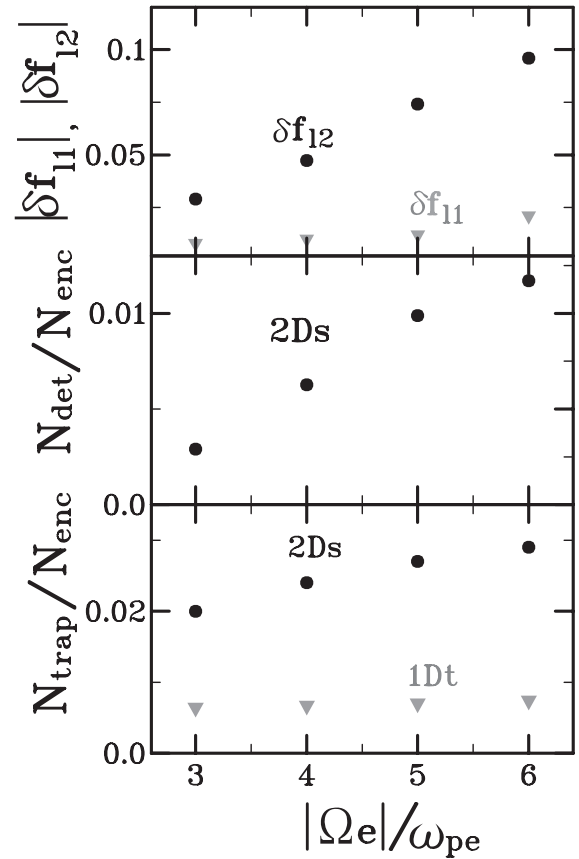


Fig. 6 Magnitudes of 1D (gray triangles) and 2D (black circles) fluctuations in the main pulse region averaged over the time period from  $\omega_{pe}t = 0$  to  $3600$ , the number of 2Ds electrons that were detrapped from the main pulse by  $\omega_{pe}t = 3600$ ,  $N_{det}$ , and the numbers of 1Dt and 2Ds electrons that got trapped in the main pulse by this time,  $N_{trap}$ , as functions of  $|\Omega_e|/\omega_{pe}$ . The values of  $N_{trap}$  and  $N_{det}$  are normalized to the number of electrons that encountered the shock wave by  $\omega_{pe}t = 3600$ ,  $N_{enc}$ .

almost equal. As for 2Ds electrons,  $N_{trap}/N_{enc}$  slightly increases with  $|\Omega_e|/\omega_{pe}$ . This is consistent with the previous result that 2D fluctuations can enhance the electron reflection near the end of the main pulse region [6].

## 4. Summary and Discussion

We studied the effects of electromagnetic fluctuations on electron motions in an oblique shock wave using 2D electromagnetic particle simulations and test particle calculations in which the equation of motion of electrons in the electromagnetic fields averaged along the shock front was computed. Comparisons of the two results confirm that 2D fluctuations along the shock front, which are excited by trapped electrons, can cause detrapping of energetic electrons from the main pulse and their subsequent acceleration to higher energies. We also studied the dependence of the electron detrapping on the external magnetic-field strength if the 1D fluctuations are small. We found that as the external magnetic field strengthens, the 2D fluc-

tuations grow to larger amplitudes, and the detrapping and subsequent acceleration of electrons enhance.

In this paper, we have studied the dependence of electron detrapping on the parameter  $|\Omega_e|/\omega_{pe}$ , setting  $v_{sh}/c \cos \theta \simeq 0.95$  and  $M_A \simeq 2.3$ . Although the value of  $\theta$  increases with  $|\Omega_e|/\omega_{pe}$ , the ratio  $N_{trap}/N_{enc}$  of the 1Dt electrons is almost independent of  $|\Omega_e|/\omega_{pe}$ , where  $N_{trap}$  is the number of trapped electrons and  $N_{enc}$  is the number of electrons that encountered the shock wave. If  $\theta$  and  $v_{sh}/c \cos \theta$  are fixed,  $M_A$  decreases with  $|\Omega_e|/\omega_{pe}$ . This indicates that if  $|\Omega_e|/\omega_{pe}$  increases, the magnitudes of the 1D fluctuations would decrease and the electron trapping would be suppressed. As for a future work, we would investigate how the electron motion in an oblique shock wave depends on  $M_A$  and  $v_{sh}$ .

## Acknowledgments

This work was carried out as part of the collaboration program under Grant No. NIFS12KNSS036 of the National Institute for Fusion Science, and of the joint research program of the Solar-Terrestrial Environment Laboratory, Nagoya University, and was supported in part by a Grant-in-Aid for Scientific Research (C) Grant No. 21540510 from the Japan Society for the Promotion of Science.

- [1] N. Bessho and Y. Ohsawa, *Phys. Plasmas* **6**, 3076 (1999).
- [2] N. Bessho and Y. Ohsawa, *Phys. Plasmas* **9**, 979 (2002).
- [3] A. Zindo, Y. Ohsawa, N. Bessho and R. Sydora, *Phys. Plasmas* **12**, 052321 (2005).
- [4] K. Shikii and M. Toida, *Phys. Plasmas* **17**, 082316 (2010).
- [5] S. Usami and Y. Ohsawa, *Phys. Plasmas* **9**, 1069 (2002).
- [6] M. Toida and J. Joho, *J. Phys. Soc. Jpn.* **81**, 084502 (2012).